Transverse modes above and below threshold in a single-frequency laser

C. J. Shackleton* and R. Loudon
Department of Physics, University of Essex, Colchester, CO4 3SQ, United Kingdom

C. A. Hill, T. J. Shepherd, M. Harris, and J. M. Vaughan
Defence Research Agency Malvern, St. Andrews Road, Malvern, Worchestire WR14 3PS, United Kingdom
(Received 24 April 1995)

We present a study of the higher-order subthreshold transverse modes in a single-frequency laser resonator. A theory is developed to describe the gain behavior when an input beam is reinjected into the laser, and tuned around the resonances that correspond to each of the subthreshold transverse modes of the cavity. Some of the predictions of the theory are confirmed by experiments with an argon-ion laser and these experiments also illustrate the use of spatial filtering for optimization of the gain, as well as an associated increase in intensity-fluctuation noise. Further experiments have been carried out to demonstrate the perturbation of the modes caused by the insertion of intracavity obstructions; the data are compared with the results from theoretical modeling of the perturbed resonator. In addition, the experimental techniques are used to track the behavior of a transverse mode as it approaches, and finally exceeds, the lasing threshold.

PACS number(s): 42.60.Jf, 42.60.Lh, 42.60.Mi, 42.79.Qx

I. INTRODUCTION

In this paper we explore the resonator-mode properties of open-sided, spherical-mirror laser cavities; we also investigate the effect on the laser modes of placing various apertures and obstructions between the mirrors. For many applications (for example, coherent laser radar) lasers are required to run on a single frequency (a single transverse mode and a single axial mode). Single-mode selection can be achieved in many ways, often readily with a homogeneously broadened active medium where only the mode with the highest gain-to-loss ratio survives the processes of mode competition. The successful single-frequency laser retains a complex spectrum of subthreshold modes: *potential* modes of oscillation that are for the moment suppressed. It is interesting, but has hitherto been difficult, to measure how well these other modes are suppressed while the laser is running. Also, we may wish to use these subthreshold modes for regenerative amplification of reflected light, choosing convenient offset frequencies and arranging the gains to be near (but not too near) threshold.

We recently reported a technique that allows the detailed study of subthreshold transverse modes including measurements of their approach to threshold [1]. The technique involves the reinjection of frequency-shifted light and has been used to study the modes of an argon-ion laser. In [1] we stressed the need for further work on the gain and noise behavior of reinjected light. Other recent work [2,3] has investigated laser amplification above and below threshold, indicating the importance of population pulsations in determining the gain spectra, but the theory did not include transverse field variations. These papers and their equations are identified by the abbreviations I and II, respectively. In this paper, we review and extend the reinjection technique, applying it to higher-order modes in a cavity perturbed in several ways; we report sensitive measurements of laser intensity-fluctuation noise and noise cancellation; and we present improved theoretical results for the form of the perturbed resonator modes and for the transverse spatial effects in the rate-equation model. The relationship of the work presented here to that covered in I and II is illustrated in Table I.

The paper is arranged in eight sections as follows. Section II reviews basic theory for the mode structure of open (possibly apertured) resonators. Section III develops the theory of gain in laser amplifiers [2,3] to include transverse effects. Section IV describes the techniques for experimental measurements of gain in transverse laser modes. Section V considers the transverse-mode contribution to laser intensity-fluctuation noise or "stochastic beam-position noise" [4]. Section VI is a theoretical and experimental study of cavity perturbation (which may appear as either friend or foe, depending on the application), and Sec. VII studies the experimental tracking of the approach to threshold under a particular mode-selecting perturbation (in this case, a thin wire). Section VIII offers an overview and some conclusions, and also reviews briefly some other related topics including higher-order modes and wideband gain in reflection.

II. MODE STRUCTURE OF OPEN RESONATORS

We first briefly review some physics and nomenclature for the stable open two-mirror resonator in Fig. 1(a) [5,6]. A *resonator mode* is a field distribution which repeats itself in shape and in phase after one round trip of the resonator. In the absence of internal apertures or perturbations, and under some simplifying paraxial assumptions, the free-space scalar wave equation has solutions in the form of pure Gaussian beams. These are the TEM_{pq} *transverse propagation modes*,

*Present address: Lumonics Ltd., Gothenburg Rd., Hull HU7 0YE, United Kingdom.

TABLE I. The work presented here is placed in context with the earlier papers I and II. The second column summarizes the scope of each paper, and the third column lists our earlier short papers on related topics.

Paper	Summary	Related papers
I (Ref. [2])	Gain and noise around the *lasing* mode. Below and above threshold. Class-*A* and -*B* laser.	[10]
II (Ref. [3])	Gain and noise around subthreshold *longitudinal* modes. Noise cancellation. Shift in spectra.	[9,14,19]
III (This work)	Study of higher-order subthreshold *transverse* modes.	[1,11]

with transverse shape given by a simple Gaussian $\exp(-r^2/w^2)$ multiplied by Laguerre polynomials (in cylindrical coordinates) or Hermite polynomials (in Cartesian coordinates). A particular set of beams can be found for given mirror curvatures R_1 and R_2, separation L, and given wavelength λ, such that the beam wave fronts coincide with the mirror surfaces and round-trip self-consistency is assured. For this set, the beam waist radius w_0 is found from

$$w_0^2 = L\lambda/\pi \sqrt{\frac{g_1 g_2 (1-g_1 g_2)}{(g_1+g_2-2g_1 g_2)^2}}, \tag{2.1}$$

and the mirrors lie at distances z_1 and z_2 from the waist:

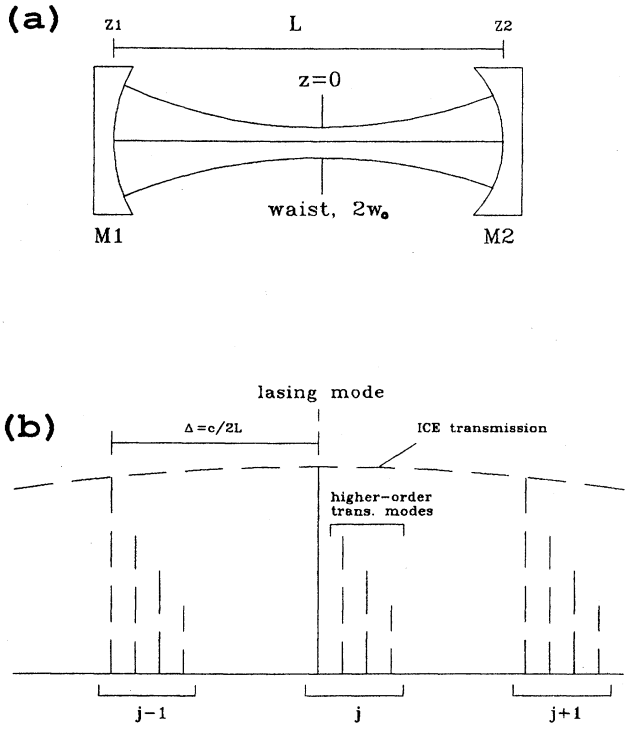

FIG. 1. (a) Schematic showing nomenclature for two-mirror open resonator. (b) Illustration of mode frequencies for the open resonator of (a). The broad curve represents the transmission envelope of a mode-selecting intracavity etalon (ICE), as for the argon-ion laser used in the experimental sections.

$$z_{1,2} = \frac{g_{2,1}(1-g_{1,2})L}{g_1+g_2-2g_1 g_2}, \tag{2.2}$$

where the resonator g parameters are defined as $g_1 = 1 - L/R_1$ and $g_2 = 1 - L/R_2$. For this set the condition $0 \leq g_1 \times g_2 \leq 1$ must be satisfied (otherwise the resonator is not "stable"). Each member of this set is then available as a distinct *transverse oscillation mode* if we supply some net round-trip gain. The cavity has a spectrum of resonant frequencies defined by

$$\frac{4\pi\nu_{j,pq}L}{c} + \Phi_{pq} = 2\pi j, \tag{2.3}$$

where j, p, and q define the mode number. The first term in (2.3) is $4\pi L$ divided by the wavelength of the light for the mode jpq, and the second term is the Guoy phase shift Φ_{pq} which depends on the transverse mode integers p and q [5]:

$$\Phi_{pq} = (p+q+1)\cos^{-1} \pm \sqrt{g_1 g_2}, \tag{2.4}$$

where the total round-trip phase shift is constrained to be an integer j times 2π. Conventionally each value of the axial mode number j is associated with its own set of transverse modes $\mathrm{TEM}_{j,pq}$. Normally in laser studies, but not necessarily, j is rather large ($\sim$10 000–100 000) and p,q rather small ($\sim$1–10); the transverse-mode shapes do not depend at all strongly on the exact value of j, and so the longitudinal- (axial) and transverse-mode effects are decoupled.

Still referring to the ideal unperturbed open resonator, we find for the mode frequencies

$$\nu_{j,pq} = c/2L\left[j + (p+q+1)\frac{\cos^{-1} \pm \sqrt{g_1 g_2}}{\pi}\right]. \tag{2.5}$$

Here, where each transverse resonator mode is a pure Gaussian beam, the extra (transverse) frequency shift is proportional to transverse-mode number [7]. This is a special property of open stable resonators, not shared by other resonators in general; for example, the phase shifts of pure transverse modes in a hollow waveguide laser scale roughly as the square of mode number. Figure 1(b) shows some of the array of equally spaced resonant frequencies.

If we now introduce an aperture or other perturbation on or between the mirrors, the resonator transverse modes will no longer be pure single TEM_{pq}; instead they will be linear combinations of TEM_{pq}, with the resonant frequencies unequally spaced. In matrix terms, if we describe the parts of the resonator by matrices $M_1, M_2, \ldots, M_n$ of TEM_{pq} cou-

pling or propagation coefficients, and obtain the transverse resonator modes as the eigenvectors of the round-trip matrix $\mathbf{M}=M_1M_2\cdots M_n$, we now have a nondiagonal $\mathbf{M}$ [7]. Later in the paper (Sec. VI) we present some results of matrix modeling for apertured resonators. In general, we are interested in $\mathbf{M}$'s eigenvectors (which give the transverse shapes of the resonator modes at a particular plane) and eigenvalues (which give the round-trip losses and relative frequencies or phase shifts). Equivalently, we may pose the resonator problem as a set of simultaneous equations, or a round-trip diffraction integral. There is a very large literature of laser resonator-transverse-mode theory, covering various numerical and analytical methods for a wide range of cavity designs, perturbations, and intracavity active media (see, for example, [6] for a review).

In the following two sections of this paper we report parallel theoretical and experimental investigations of the subthreshold mode structure of a double-ended argon laser: that is, we probe the cavity to measure the behavior (in frequency and space) of resonator modes that are *potential* modes of oscillation but are for the moment suppressed by competition from one lasing mode with higher gain-to-loss ratio. We reinject a portion of the laser output into one end of the laser, with some offset frequency, and measure the signal generated when the output from the other end falls on a square-law envelope detector. This latter output may be expressed as the sum of (i) radiation in the lasing mode and (ii) radiation which is offset in frequency, present in some linear combination of transverse modes, and *regeneratively amplified* after reinjection. The degree of amplification may be very sensitive to the reinjected signal's frequency and spatial form, but we will assume initially that this signal is very *weak* and does not perturb the lasing process (we will examine later some effects of coupling and transverse-mode interaction). Hence the detector sees essentially a steady laser output at fixed frequency acting as a local oscillator, plus an independent weak signal at a single (tunable) frequency. The detector output contains an ac component (i.e., a beat) at the difference frequency with amplitude proportional to

$$\int\int E_{\mathrm{sig}}(x,y)E_{\mathrm{LO}}(x,y)dx\,dy, \tag{2.6}$$

where the integral is carried out over the detector surface. Now it is found that, to good approximation, the resonator transverse modes of the cavities considered here are *spatially orthogonal*: for any two different modes (each a linear combination of TEM_{pq}) this integral across the complete transverse plane is near to zero. In our experiments, however, the area of integration may be artificially restricted by finite detector size or by convenient apertures in order to enhance the contribution from certain resonator-mode spatial components of E_{sig} and hence yield a nonzero beat. In particular, if two higher-order transverse modes have nearly equal resonant frequencies, then their contributions to regenerative amplification may be individually resolved by appropriately aperturing the detector or the beam. We demonstrate here these important orthogonality properties both for reinjected single-frequency light and for the noise due to amplified spontaneous emission. It should be noted that there is a large subliterature on the mathematical and experimental validity of these properties; in particular, the zero integral is strictly true only for two biorthogonal or adjoint modes [8], and there has been considerable discussion of the breakdown of orthogonality in more exotic and unstable resonators. In practice, at a lesser level of rigor, we find that models based on the usual approximations for TEM_{pq} basis modes produce accurate orthogonality, and that careful experiments produce very low beat strengths for different modes.

In summary, a transverse mode of *propagation* must satisfy the appropriate wave equation with transverse boundary conditions. A transverse mode of *oscillation* additionally satisfies the round-trip shape self-consistency condition for its cavity. The term *resonator mode* usually implies an actual or potential oscillation, described by transverse-mode numbers, an axial-mode number, and a frequency $\nu_{j,pq}$.

Having presented these well-known principles of resonator mode structure — the shapes, relative phase shifts, and Gaussian-beam description of the potential oscillating modes in Fig. 1 — we will return to them in Secs. VI, VII, and VIII when describing the predicted and observed effects of cavity perturbations. First, we extend our previous treatment of laser amplification and reinjection by adding, at least to a crude approximation, a transverse spatial term (Sec. III).

III. THEORY OF TRANSVERSE-MODE GAIN

A. Laser amplifier equations of motion

We need to calculate the gain experienced by an input signal of the form

$$\beta_{\mathrm{in}}=\beta_s\,\exp[-i(\omega_L+\omega)t]. \tag{3.1}$$

Here β_{in} is proportional to the E field of the input signal expressed in units such that $|\beta_{\mathrm{in}}|^2$ is the input energy flux in photons per second, ω_L is the frequency of the lasing mode, assumed to be the lowest-order (TEM_{00}) transverse mode, and the detuning ω is chosen so that $\omega_L+\omega$ lies within the frequency spread of the subthreshold higher-order transverse mode centered on ω_T (ω_T is used here as shorthand for $\omega_{j,pq}=2\pi\nu_{j,pq}$). The spatial distribution of the input signal is assumed to be matched to that of the subthreshold transverse mode under investigation. Note that this assumption is not generally fulfilled in our experiments described in Sec. IV. In that case, it is only the projection of the input field onto the mode of interest that contributes to the measured gain. The theory here assumes a matched input to allow calculation of absolute values for the gain.

The required theory can be developed by extension and modification of our previous work [2,3] on the gain at frequencies within the lasing mode (I) and at frequencies close to the subthreshold longitudinal modes on either side of the laser mode (II). The present calculation resembles that of II, with the introduction of the input signal (3.1) causing new components in the system dynamics at the signal frequency $\omega_L+\omega$ and its "image" $\omega_L-\omega$, in addition to the frequency ω_L of the free-running laser. However, in contrast to the symmetrical disposition of adjacent longitudinal (TEM_{00}) modes around the lasing mode, there is in general no mode

of the cavity at the image frequency $2\omega_L-\omega_T$ [see Fig. 1(b)]. Thus any tendency of the atoms to generate light at this frequency is heavily inhibited, and to first order in the signal amplitude β_s the field α in the laser cavity has the two-component form

$$\alpha=\alpha_L \exp(-\omega_L t)+\alpha_T \exp[-i(\omega_L+\omega)t]. \quad (3.2)$$

Here α_L is the intracavity E field of the free-running laser, expressed in units such that $|\alpha_L|^2$ is the mean number of laser photons in the cavity, and α_T is the corresponding field amplitude appropriate to the subthreshold transverse mode with injected input. The presence of simultaneous signal and image contributions to the gains studied in I and II led to striking cancellation effects which are absent in the present problem.

The atomic medium that drives the laser is described by two variables, the mean collective atomic dipole moment d and the mean population inversion D. The dipole moment has the three-component form

$$d=d_L \exp(-i\omega_L t)+d_T \exp[-i(\omega_L+\omega)t] + d_I \exp[-i(\omega_L-\omega)t], \quad (3.3)$$

where the final component, at the image frequency, is unable to generate a corresponding cavity field as described above. In modeling the dynamics of the population inversion, it is important to take account of the different distributions of intensity in the TEM_{00} lasing mode and the subthreshold higher-order transverse mode in the planes perpendicular to the cavity axis. These different distributions cause the two modes to interact with sets of atoms that are to some extent shared but are to some extent distinct. In a rough approximation to the complicated variation of mode intensity and overlap in the perpendicular planes, we assume that the pumped population D_p of inverted atoms in interaction with the cavity field (3.2) has a fraction f_L that is coupled to the lasing mode and a fraction f_T that is coupled to the transverse mode ($0\leq f_L, f_T\leq 1$). There are thus three distinct values of the atomic population inversion D, as follows: (i) for the fraction $1-f_T$ interacting solely with the lasing mode, $D=D_L$, (ii) for the fraction $1-f_L$ interacting solely with the transverse mode, $D=D_T$, and (iii) for the fraction f_L+f_T-1 interacting with both modes, where the relevant population inversion is driven to pulsate at the difference of their frequencies and we put

$$D=D_0+D_1 \exp(-i\omega t)+D_1^* \exp(i\omega t). \quad (3.4)$$

Two special cases of the mode fractions occur when both modes interact with all inverted atoms,

$$f_L=f_T=1, \quad (3.5)$$

or the modes interact with completely distinct sets of inverted atoms,

$$f_L+f_T=1. \quad (3.6)$$

We note that the subthreshold longitudinal- (TEM_{00}) mode problem treated in II corresponds to the special case (3.5), for which only the third component of the population inversion given by (3.4) survives, and its form is the same as that of II (2.4).

The laser equations of motion are similar to I (2.6)–(2.8), the conventional Maxwell-Bloch equations. The separated equations of motion for the two components of the cavity field (3.2) are

$$\dot{\alpha}_L+(\gamma_L+i\omega_L)\alpha_L=g d_L, \quad (3.7)$$

$$\dot{\alpha}_T+(\gamma_T+i\omega_T)\alpha_T=g d_T+\gamma_{\rm in}^{1/2}\beta_{\rm in}, \quad (3.8)$$

where γ_L and γ_T are the damping rates for the two modes and $\gamma_{\rm in}$ represents the cavity mirror intensity transmission coefficient for the input signal. Generally the condition $\gamma_T\alpha_T>g d_T$ ensures that the transverse mode remains below threshold.

For the atomic variables, the decay rate $\gamma_\perp$ associated with the atomic dipole moment is assumed to give rise to a high degree of homogeneous broadening, sufficient to permit the neglect of inhomogeneous effects such as Doppler broadening (see Sec. I of II). In addition, $\gamma_\perp$ is sufficiently large for class-A and class-B lasers that an adiabatic approximation can be made in the equation of motion for d, resulting in the form given in I (2.15),

$$\gamma_\perp d=g\alpha D. \quad (3.9)$$

The validity of this approximation is fully discussed in I and II, and the separation of (3.9) into components that oscillate at the three frequencies occurring in (3.3) gives the relations

$$d_L=g\alpha_L(D_0+D_L)/\gamma_\perp, \quad (3.10)$$

$$d_T=g\{\alpha_L D_1+\alpha_T(D_0+D_T)\}/\gamma_\perp, \quad (3.11)$$

$$d_I=g\alpha_L D_1^*/\gamma_\perp. \quad (3.12)$$

The variables α_T and D_1 are proportional to the signal amplitude $\beta_{\rm in}$ and results are given correct to first order in $\beta_{\rm in}$ here and subsequently, so that the final expression for the gain is restricted to the regime of linear amplification.

The equation of motion for the atomic population inversion is identical to I (2.7) in the form

$$\dot{D}+\gamma_\parallel D=\gamma_\parallel D_p-g(\alpha^* d+\alpha d^*), \quad (3.13)$$

where the population of the lower atomic level of the laser transition is assumed to be negligible compared to that of the upper level. Here $\gamma_\parallel$ is the atomic longitudinal decay rate and D_p is the total population of inverted atoms in the absence of any cavity field, proportional to the laser pumping rate. The separation of (3.13) into its different frequency components is accompanied by the division of the atomic population into the fractions that interact with the different cavity modes. The resulting equations of motion are

$$\gamma_\parallel D_L=\gamma_\parallel(1-f_T)D_p-g(\alpha_L^* d_L+\alpha_L d_L^*)\frac{1-f_T}{f_L}, \quad (3.14)$$

$$\gamma_\parallel D_T=\gamma_\parallel(1-f_L)D_p, \quad (3.15)$$

$$\gamma_{\parallel} D_0 = \gamma_{\parallel}(f_L + f_T - 1) D_p - g(\alpha_L^* d_L + \alpha_L d_L^*) \frac{f_L + f_T - 1}{f_L}, \tag{3.16}$$

$$D_1 + \gamma_{\parallel} D_1 = -g(\alpha_L^* d_T + \alpha_L d_I^*) \frac{f_L + f_T - 1}{f_T} - g \alpha_T d_L^* \frac{f_L + f_T - 1}{f_L}, \tag{3.17}$$

again correct to first order in β_{in}. Note that the divisions by f_L or f_T in three of these equations are needed to convert forces that drive all of the atoms illuminated by a given mode into the three subsets of these atoms defined earlier.

With the dipole-moment components removed by the use of (3.10)–(3.12), the set of six equations (3.7), (3.8), and (3.14)–(3.17) provides solutions for the six variables α_L, α_T, D_L, D_T, D_0, and D_1.

B. Free-running laser

In the absence of an input signal, $\beta_{\text{in}} = 0$, the variables α_T and D_1 vanish, and the Maxwell-Bloch equations simplify considerably. Thus the field equation (3.7) becomes

$$\gamma_L \alpha_L = g^2 \alpha_L (D_0 + D_L)/\gamma_{\perp}, \tag{3.18}$$

where (3.10) has been used, while the population inversion equations (3.14) and (3.15) similarly become

$$\gamma_{\parallel} D_L = \{\gamma_{\parallel} f_L D_p - (g^2/\gamma_{\perp}) 2 |\alpha_L|^2 (D_0 + D_L)\}(1 - f_L)/f_L, \tag{3.19}$$

$$\gamma_{\parallel} D_0 = \{\gamma_{\parallel} f_L D_p - (g^2/\gamma_{\perp}) 2 |\alpha_L|^2 (D_0 + D_L)\} \times (f_L + f_T - 1)/f_L. \tag{3.20}$$

The above-threshold solutions of these three equations are obtained straightforwardly. Thus the laser field amplitude is given by

$$|\alpha_L|^2 = (C - 1) n_s, \tag{3.21}$$

where the cooperation parameter is defined to be

$$C = g^2 f_L D_p / \gamma_L \gamma_{\perp} \tag{3.22}$$

and the saturation photon number is

$$n_s = \gamma_{\perp} \gamma_{\parallel} / 2 g^2. \tag{3.23}$$

Two components of the population inversion are obtained from (3.18)–(3.20) as

$$D_L = \frac{\gamma_L \gamma_{\perp}}{g^2} \frac{1 - f_T}{f_L}, \tag{3.24}$$

$$D_0 = \frac{\gamma_L \gamma_{\perp}}{g^2} \frac{f_L + f_T - 1}{f_L}, \tag{3.25}$$

independent of the laser pumping rate. A third component of the population inversion is obtained from (3.15) as

$$D_T = (1 - f_L) D_p = C \frac{\gamma_L \gamma_{\perp}}{g^2} \frac{1 - f_L}{g_L}. \tag{3.26}$$

In contrast to the other two, this component is proportional to the pumping rate, a consequence of the below-threshold character of the transverse mode [compare I (3.4)].

C. Transverse gain

An expression for the transverse gain is obtained by solution for α_T of the so-far unused Maxwell-Bloch equations (3.8) and (3.17). The procedure is to remove the dipole-moment components with the use of (3.10)–(3.12), to remove the laser-field amplitude with the use of (3.21), and to remove three components of the population inversion with the use of (3.24)–(3.26). The two remaining equations now involve only the variables α_T and D_1. Elimination of the latter provides the desired expression for α_T. The calculation is algebraically very tedious but essentially straightforward and we present only its final result. The intensity gain for transmission through the laser amplifier cavity at signal detunings ω close to

$$\delta_T = \omega_T - \omega_L \tag{3.27}$$

is defined to be

$$G_T = \gamma_{\text{out}} |\alpha_T / \beta_{\text{in}}|^2, \tag{3.28}$$

where γ_{out} represents the laser cavity mirror transmission coefficient for the amplified output signal. The gain profile can be written in Lorentzian form as

$$G_T(\omega) = \frac{\gamma_{\text{in}} \gamma_{\text{out}}}{(\omega - \delta_T - S_T)^2 + (\Gamma_T/2)^2}, \tag{3.29}$$

where the shift and width are given by

$$S_T = \frac{\delta_T \gamma_L \gamma_{\parallel} (C - 1)[(C - 1)(1 - f_L) + 2 f_T](f_L + f_T - 1)/2 f_L f_T}{\delta_T^2 + (\gamma_{\parallel}/f_T)^2 [(C - 1)(f_L + f_T - 1) + f_T]^2} \tag{3.30}$$

and

$$\Gamma_T = \frac{\gamma_L \gamma_{\parallel}^2 (C - 1)[(C - 1)(f_L + f_T - 1) + f_T][(C - 1)(1 - f_L) + 2 f_T](f_L + f_T - 1)/f_L f_T^2}{\delta_T^2 + (\gamma_{\parallel}/f_T)^2 [(C - 1)(f_L + f_T - 1) + f_T]^2} + 2\gamma_T - 2(\gamma_L/f_L)[(C - 1)(1 - f_L) + f_T]. \tag{3.31}$$

These somewhat complicated expressions simplify considerably for the special cases defined in (3.5) and (3.6). Thus, in the case where the lasing mode and the transverse mode both interact with the complete population of inverted atoms, (3.30) and (3.31) reduce to

$$S_T=\frac{\delta_T\gamma_L\gamma_{\parallel}(C-1)}{\delta_T^2+C^2\gamma_{\parallel}^2} \quad (f_L=f_T=1) \tag{3.32}$$

and

$$\Gamma_T=\frac{2\gamma_L\gamma_{\parallel}^2(C-1)C}{\delta_T^2+C^2\gamma_{\parallel}^2}+2\gamma_T-2\gamma_L \quad (f_L=f_T=1). \tag{3.33}$$

These expressions are similar to the shift and the width found in II (2.30) and (2.31) for the gain associated with adjacent subthreshold longitudinal modes that share the same atomic population with the lasing mode. In the opposite extreme, where the lasing mode and the transverse mode interact with totally distinct sets of atoms, the complete gain profile (3.29) reduces to

$$G_T(\omega)=\frac{\gamma_{\text{in}}\gamma_{\text{out}}}{(\omega-\delta_T)^2+\gamma_T^2(1-C_T)^2} \quad (f_L+f_T=1), \tag{3.34}$$

where

$$C_T=g^2f_TD_p/\gamma_T\gamma_{\perp} \tag{3.35}$$

is the same as the cooperation parameter (3.22) but with the lasing-mode parameters replaced by transverse-mode parameters. The gain profile (3.34) is similar to that derived in I (4.6) for a single subthreshold (TEM_{00}) longitudinal mode. However, it should be emphasized that the theory developed in the present section applies to a laser in which only the single TEM_{00} mode is above threshold. Thus the gain expression (3.34) is valid only when the transverse cooperation parameter (3.35) is less than unity, and this condition is easily violated for very reasonable values of the various laser parameters, as is demonstrated by some of the numerical results for the more general gain expression (3.29) discussed below. Furthermore, it will be demonstrated in the next section that the observed gain around a subthreshold transverse mode is only fully measured when the laser input and output are correctly spatially filtered. Without filtering, the beat signal in the output is highly suppressed due to orthogonality between the lasing mode and the threshold transverse mode.

Some examples of the variation of transverse shift with cooperation parameter C obtained from (3.30) are shown in Fig. 2, where the units are converted from angular frequency to MHz and the values of $\gamma_{\parallel}$ and γ_L are those measured in earlier work on the same laser (papers I and II). The three parts of the figure refer to the transverse modes that were experimentally investigated in detail for an argon-ion laser, to be discussed in Sec. IV. For the want of any precise knowledge of the transverse distributions of optical intensity in these modes, it is assumed that the fractions f_L and f_T of pumped atoms with which they interact are equal. It is seen that the shifts tend to increase with the detuning of the higher-order transverse mode from its TEM_{00} counterpart.

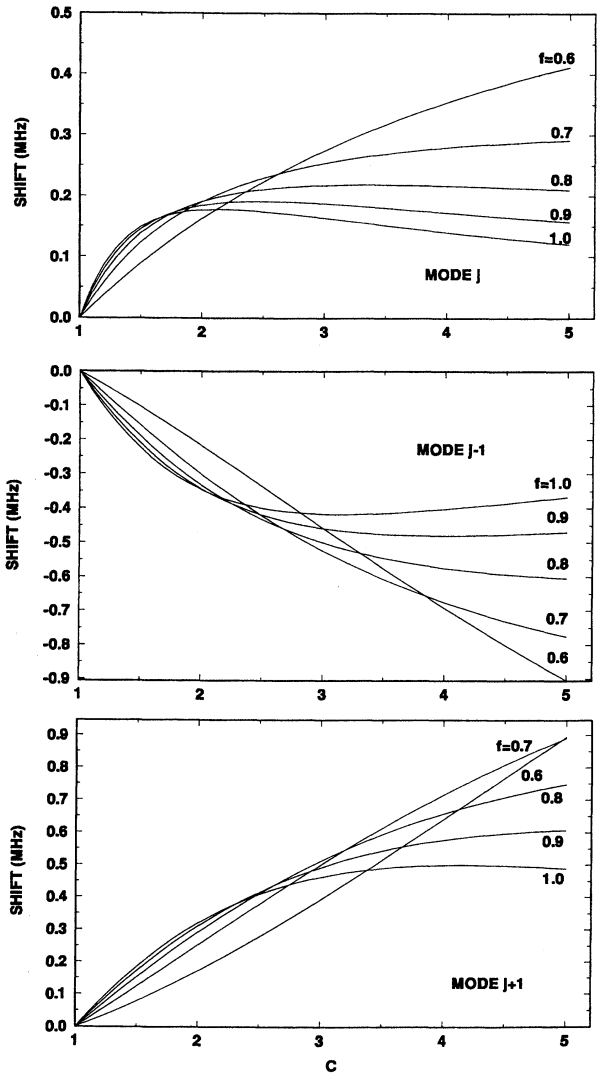

FIG. 2. Frequency shift of transverse modes away from the lasing (TEM_{00}) mode, computed from Eq. (3.30) as a function of the cooperation parameter C. The laser parameter values are chosen as appropriate to the argon-ion system of Sec. IV: $\gamma_{\parallel}=4.0\times10^8\ s^{-1}$, $\gamma_L=8.7\times10^6\ s^{-1}$. The laser power is proportional to $C-1$, and $C=2$ corresponds to an output of 5.5 mW. The top graph represents the modes TEM_{01} and TEM_{10} with the same longitudinal-mode number (j) as the lasing mode, and detuned from it by approximately 35 MHz. The other two graphs represent the same transverse modes, but with longitudinal numbers $j-1$ and $j+1$. These modes have approximate detunings of -121 MHz and 191 MHz, respectively (see Fig. 1). For each mode, curves are plotted for atomic fractions $f=f_L,f_T$ running from 0.6 to 1.

For a given transverse mode, the magnitudes of the shifts at low powers ($C<2$) are larger for larger values of the atomic fractions $f_L=f_T$. The shift increases quite rapidly as C increases from unity but levels off or even diminishes for the larger values of C. Note that the shift tends to zero as the fractions f_L and f_T tend to the value 0.5, indicating no spatial overlap between the lasing mode and the transverse mode

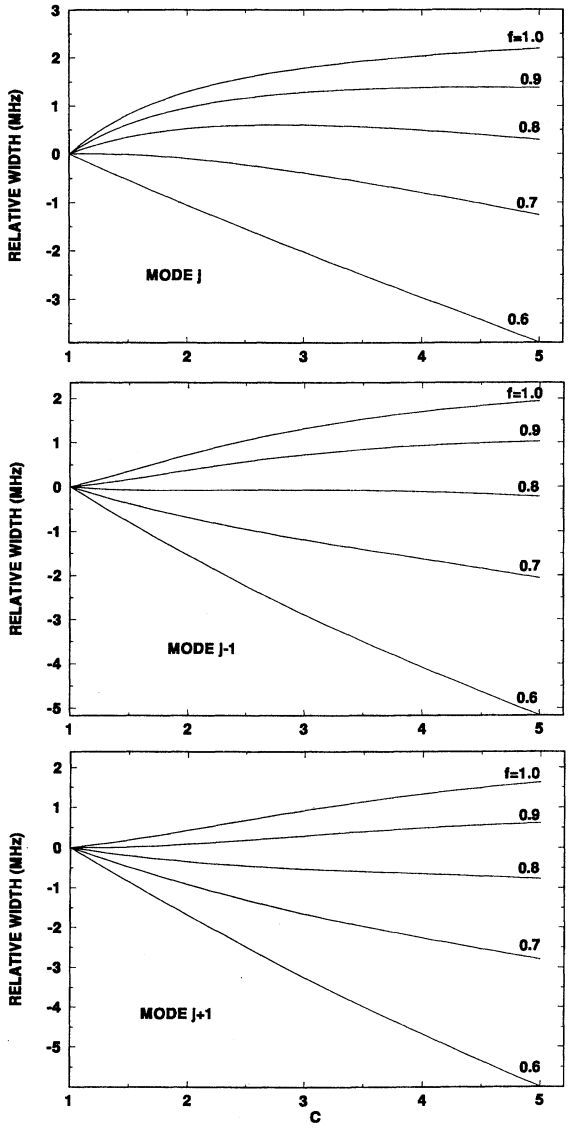

FIG. 3. Relative width $\Gamma_T - 2\gamma_T + 2\gamma_L$ of the transverse modes, computed from Eq. (3.31) as a function of C. All parameters take the same values as in Fig. 2. Note that a negative relative width simply implies a *reduction* in mode width from the initial passive-cavity value. If this reduction exceeds the initial value, the implication is that the mode has passed its lasing threshold.

under consideration. Such conditions result in independent operation of the two modes with no interaction. A direct comparison between theory and the experimental results of the next section gives poor agreement. However, agreement between the two can be restored by adding to the theoretical curves a monotonically increasing positive shift that reaches a value in the range 0.5–0.8 MHz at $C=5$. Such a shift may be accounted for by the distortion of transverse-intensity profiles with increasing laser power as the modes forage for the most abundant provision of inverted atoms.

The corresponding variations of transverse linewidth obtained from (3.31) are shown in Fig. 3, where the quantity

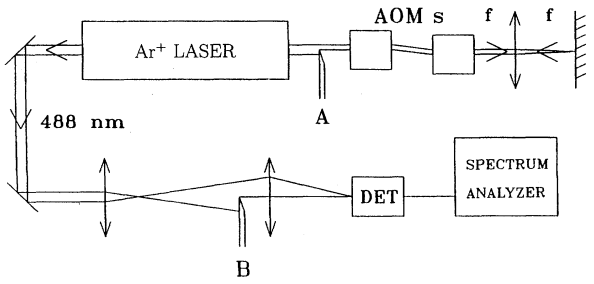

FIG. 4. Experimental arrangement for the study of subthreshold transverse modes. One output beam from the double-ended argon-ion laser is shifted by tunable acousto-optic modulators (AOM) and reinjected into the laser cavity. The output from the other end is incident on a detector (DET). A and B are knife-edge blades for spatial filtering of input and output, respectively. Their orientation determines which transverse mode is probed.

plotted is $\Gamma_T - 2\gamma_T + 2\gamma_L$, again in MHz. The linewidths decrease with decreasing atomic fractions $f_L = f_T$, as the transverse modes increasingly interact with their own exclusive atoms and thereby acquire the ability to approach lasing threshold. The thresholds occur when $\Gamma_T = 0$, but the corresponding values of C cannot be obtained directly from Fig. 3 since $\gamma_T > \gamma_L$ and the values of γ_T are not known for the transverse modes observed in our experiments. Nevertheless, it is seen from Fig. 3 that the oscillation threshold is reached for smaller values of C as the transverse-mode detuning increases and as the atomic fractions decrease.

IV. EXPERIMENTAL MEASUREMENTS OF GAIN IN TRANSVERSE LASER MODES

In this section, we describe a straightforward and generally applicable technique that allows the accurate and detailed study of subthreshold spatial modes of a cw single-frequency laser. Some preliminary results were described previously in a short Letter [1]. The technique is based on measurements of the amplification of frequency-shifted light that has been injected into the laser cavity [1,3,9–11]. In the simplest terms, an enhanced gain at a particular frequency is taken to indicate the presence of a subthreshold mode. However, we will show later that there are some complications to the analysis of the data; the theory for the gain described in Sec. III revealed that the peak gain does not necessarily coincide precisely with the mode centre. Nevertheless, it will be demonstrated that the technique allows information to be obtained straightforwardly on the mode resonance frequencies, as well as on proximity to threshold.

The data reported here have been obtained with a double-ended single-frequency argon-ion laser, running on the TEM_{00} mode. The laser cavity mirrors ($M1$ and $M2$) are set approximately 1.0 m apart, giving a longitudinal-mode spacing $\Delta = 156.02$ MHz. Two resonator arrangements have been examined, consisting firstly of one plane mirror and one concave, and secondly of two concave mirrors. The mirror transmissivities are each of order 5%, and all values of laser power here refer to the emission from one end only. The laser has an intracavity etalon to ensure operation on a single

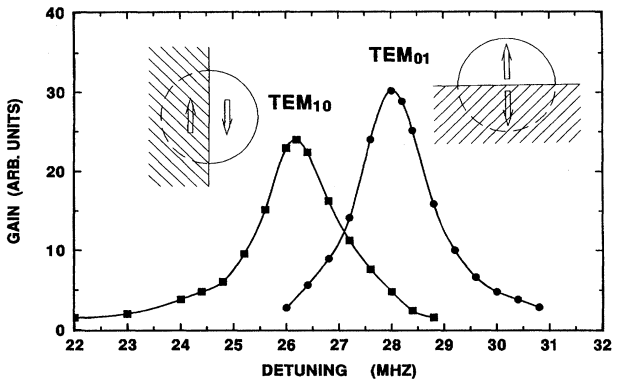

FIG. 5. Typical gain profiles for the TEM_{01} and TEM_{10} modes of the argon-ion laser sharing the same longitudinal-mode number as the lasing (TEM_{00}) mode. The cavity uses a plane-concave mirror pair [case (i)]. The detuning is always positive. The spatial filtering of the output laser beam appropriate to each measurement is also indicated.

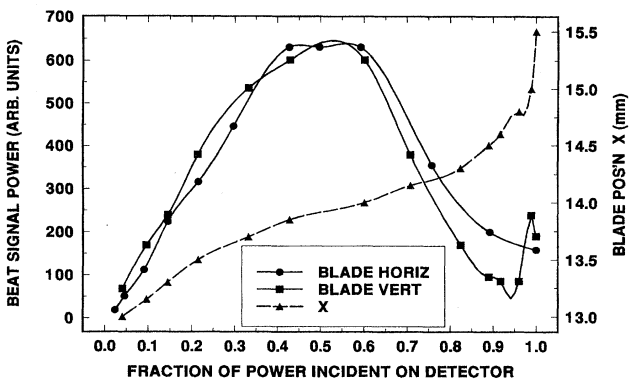

FIG. 6. Signal strength at the peak of the gain curve for TEM_{01} and TEM_{10} modes as the knife-edge blade (B in Fig. 4) is translated into the laser output beam. Also plotted is the laser power incident on the detector versus blade position. The laser power is fixed throughout at 15 mW. There is some distortion to the curves due to minor inhomogeneities in the detection system: these are more evident when the detector is exposed to the majority of the beam (right-hand side of the plot).

longitudinal mode [3]. Further details of the laser parameters may be found in [2] and [3]. In our experiments (Fig. 4), the output beam from one end of the laser passes through a pair of acousto-optic modulators. In double pass, this allows a precise shift δ of the beam's frequency anywhere in the range $0-\pm 350$ MHz. The shifted beam is then reinjected into the laser cavity; the output from the other end of the laser displays a beat at the difference frequency δ and the strength of this beat is taken (as in I and II) to be a measure of the gain experienced by the reinjected beam. This gain, as expressed in (3.28), shows a marked resonance peak when tuned around the vicinity of a subthreshold transverse mode. The input is normally heavily attenuated to avoid disturbing the laser; with only 10^{-5} of the power returned to the cavity, the gain measurements typically have a signal-to-noise ratio of $>10^3$. Some of the nonlinear and injection-locking phenomena that occur when the input signal exceeds the small-signal limit are discussed briefly in [11], which studies these effects in a CO_2 waveguide laser. Because of the orthogonality of transverse modes, the beat signal may be greatly increased by appropriate spatial filtering of both the input and output beams. As discussed earlier, such filtering also acts as a discriminant between nearly degenerate modes.

As an example, Fig. 5 presents gain data for the first-order Hermite Gaussian TEM_{01} and TEM_{10} modes[1] (with mirror $M1$ plane, mirror $M2$ concave). These modes have their frequency degeneracy split by the astigmatism that components such as Brewster windows introduce into the cavity [7,12]. The Brewster windows are oriented so as to polarize the laser with its E vector vertical; under this condition, the lobes of the transverse modes are aligned along vertical and horizontal axes for TEM_{01} and TEM_{10}, respectively. Initially we will assume symmetrical, unperturbed modes (that is, *strictly* pure TEM_{pq}); the effects of perturbation will be investigated in Secs. VI and VII. The beat signal power (taken to be proportional to gain) is measured by spectral analysis of the output current from the detector, and its strength for these modes is maximized by blocking precisely half of the laser beam power at both the input and output (Fig. 4). This destroys the symmetry that, for transverse modes orthogonal to the lasing TEM_{00} mode, leads to cancellation of the contributions to the gain from the two halves of the beam. Blocking half the beam with vertical knife-edge blades maximizes the signal from the TEM_{10} mode; horizontal blades select the TEM_{01} mode. Figure 6 shows the variation of the signal at the peak of the gain curve for these two modes, as the blade is translated so as to block a progressively larger fraction of the detected laser beam. The maximum signal is seen to occur when exactly half the power of the laser beam is passed by the blade. A further fourfold increase in signal power could be achieved by employing a split-detector arrangement [4] in which the two halves of the beam are separately detected, and their respective photocurrents added in antiphase. In comparison to this filtering of the *output*, the signal power is less sensitive to the spatial filtering of the *input*: there is no need for accurate mode matching of the signal beam with the desired transverse mode because the predetection filtering ensures that only this mode contributes to the signal. Any other transverse modes of the laser that may become excited by the input do not contribute because of orthogonality.

The two gain profiles for the reinjected light plotted in Fig. 5 clearly show the frequency splitting due to astigmatism to be about 2 MHz. The detunings δ in the measurements of Fig. 5 are always positive, confirming that the transverse modes have a higher frequency than the TEM_{00} mode with identical axial-mode number. Enhanced gain can also be observed for negative δ at frequencies around $\delta=-(\Delta-27)$ MHz, as this probes the TEM_{01} and TEM_{10} modes with their longitudinal (axial) mode number reduced by one (see Fig. 1). Similarly, other axial orders may be probed by adding or subtracting multiples of Δ (≈ 156

[1]We use this labeling throughout with the caveat that the modes are not necessarily always of pure Hermite Gaussian form.

MHz) to the detuning. We now present a more systematic study of the properties of the two lowest-order transverse modes, TEM_{01} and TEM_{10}. More specifically, the mode frequencies and the gain spectra have been examined here as functions of mirror curvature, laser power, and longitudinal-mode number.

A comparison between the mode frequencies for mirror sets of different curvature allows a simple check of correct transverse-mode behavior. An increase in the degree of curvature encourages the laser modes to have a narrower waist and greater divergence. This leads, in general, to an increased spacing between the fundamental (TEM_{00}) mode and the higher-order transverse modes, as may be seen from (2.5). We have made measurements of this splitting for the two cavity configurations mentioned earlier; the laser was set up (i) with a plane mirror $M1$ and concave mirror $M2$ (radius $r=4.1$ m), and (ii) with concave $M1$ ($r=5.1$ m) and concave $M2$ ($r=4.1$ m). The frequency separation of the TEM_{01} and TEM_{10} modes from the fundamental may be estimated from (2.5). This ignores any perturbations such as might result from an inhomogeneous gain medium, Brewster windows, and edge effects at the mirrors and the discharge bore. Equation (2.5) predicts splittings of 25.4 and 33.6 MHz for cases (i) and (ii), respectively. This is in good agreement with observation; the data of Fig. 5 [case (i)] show the average splitting for the TEM_{01} and TEM_{10} modes to be about 27 MHz and the corresponding splitting for case (ii) was found to be about 35 MHz. These measured values are thus slightly higher than the theoretical ones, and it is likely that this is a result of the various distortions and perturbations to the cavity mode just mentioned. For the more detailed studies presented in the remainder of this section, the laser had two concave mirrors [case (ii)].

It has been assumed throughout the above analysis that the mode frequency may be accurately identified from the peak of the mode's gain curve. However, the theoretical results of the previous section indicate that there is generally a frequency shift given by (3.30) which leads to a small discrepancy between these two values. We next demonstrate experimental measurements of frequency shift. The frequency of peak gain will be shown to vary with laser power, and two distinct contributions to this shift will be identified. First, as shown in Sec. III, the gain curve becomes "pulled" to higher frequency by the influence of oscillations of the inversion ("population pulsations" [2,3,13]) at the beat frequency. Secondly, the gain medium usually acquires a nonuniform distribution, and this inhomogeneity varies with power because of changing discharge conditions and/or spatially selective gain saturation. This results in the distortion of the transverse resonator modes, and their frequencies are shifted accordingly. This effect was neglected in the theoretical treatment of gain in Sec. III. It is, however, possible to decouple these two contributions by observing gain profiles for different longitudinal values of the same transverse mode (see Fig. 1). For modes on the high-frequency side of the lasing mode, the two effects mentioned above act in the same direction, whereas on the low-frequency side they oppose each other.

In Fig. 7 we plot the experimental measurements of the frequency shifts of the peak gains for the TEM_{01} and TEM_{10} modes as functions of laser power. The reinjection technique permits such data to be gathered quickly and easily. Note the significant differences in behavior for the different values of longitudinal-mode number, particularly for modes on opposite sides of the lasing mode. Not surprisingly, in each case the TEM_{01} and TEM_{10} modes show very similar responses.

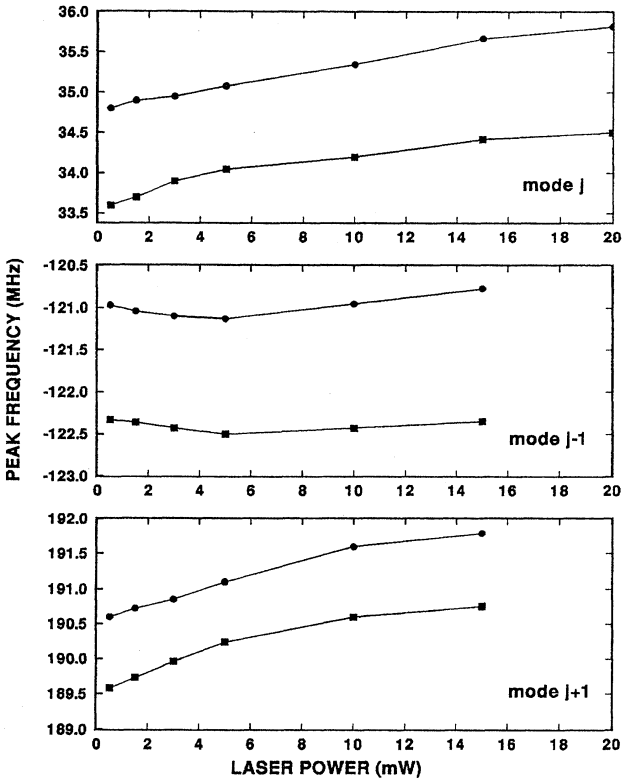

FIG. 7. Plot of position of the peak of the gain curve versus laser power for the TEM_{01} and TEM_{10} modes at three values of longitudinal mode number (i.e., $j-1$, j, and $j+1$, where j is that for the lasing mode). Squares: TEM_{10}. Circles: TEM_{01}. In this case, the cavity uses a concave-concave mirror pair [case (ii)].

In order to make a direct quantitative comparison between the data of Fig. 7 and the theoretical predictions for the shift in Sec. III (Fig. 2) it is necessary to eliminate the contribution from the mode distortion, as this contribution was ignored by the theory. This is most conveniently done by comparing the differences in the values of shift for transverse modes that differ only by their value of longitudinal-mode number j. The mode distortion is assumed to be independent of longitudinal-mode number, since the effect only involves transverse variations of the gain medium. This results from the "decoupling" of axial and transverse effects mentioned in Sec. II, giving rise to the repeating comb of mode frequencies in Fig. 1(b). Hence the contributions to the shift from mode distortion cancel in the values of differential shift. These values therefore only contain the shifts due to population pulsation, and are plotted in Fig. 8, together with the corresponding theoretical values, making the same assumptions about the parameter values that were used in Sec. III. While three possible sets of values of the differential shift exist for the data in Fig. 7, only two of these sets contain

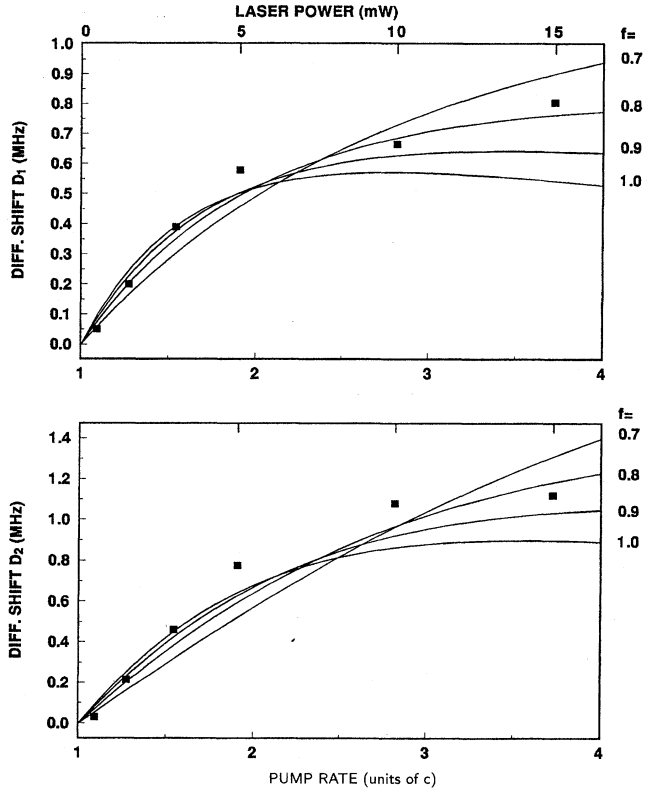

FIG. 8. Comparison between theory and experiment for differences in frequency offset. Differential shift $D1$ is defined as $S_T(j)-S_T(j-1)$, and $D2$ is defined as $S_T(j+1)-S_T(j-1)$, where j denotes the longitudinal-mode number of the lasing mode. The results are the mean values for the TEM_{01} and TEM_{10} modes, and it is assumed that $f_L=f_T=f$.

independent information; accordingly just two have been selected for display in Fig. 8.

Considering the simplistic approximations that have been made in the theory of Sec. III, the agreement is remarkably good. The value of the atomic fractions (f_L,f_T) are most likely to lie in the range 0.7–0.9, and it is possible that they could alter with laser power. Therefore these theoretical curves should be considered roughly to define an envelope of possible values for the experimental data. It must be stressed that the theory contains no additional floating parameters, all other values having been determined by the previous experiments reported in I and II. The widths of the gain curves were also found to be consistent with the predictions shown in Fig. 3, but no detailed measurements were made to allow a quantitative comparison.

V. TRANSVERSE-MODE CONTRIBUTION TO LASER INTENSITY-FLUCTUATION NOISE

In I and II, much emphasis was placed on the intensity-fluctuation noise properties of the laser resulting from spontaneous emission into the lasing mode (I) and the adjacent subthreshold longitudinal modes (II). Spontaneous emission into the subthreshold transverse modes considered here also

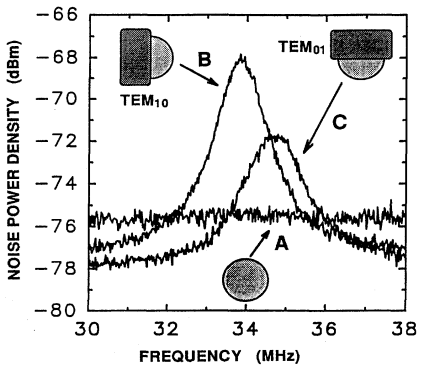

FIG. 9. Intensity-fluctuation noise spectrum of the complete output beam in the region of the subthreshold TEM_{01} and TEM_{10} modes (curve A). Curves B and C show the corresponding noise spectra when the output is spatially filtered by blocking half of the laser power with a knife-edge blade. Note the reduction by 3 dB (i.e., a factor of 2) in the shot-noise level. Vertical and horizontal filtering reveals the TEM_{10} and TEM_{01} noise spectra, respectively. The difference between the peak noise levels in the two cases is not fully understood. It appears sensitive to the cavity mirror alignment: compare and contrast with the peak heights of Fig. 5.

has implications for the laser intensity noise, but in this case the noise is only revealed after spatial filtering of the output. In this section, we briefly review the noise phenomena associated with the transverse modes and present data which confirm the close relationship between gain and noise.

Figure 9 shows different intensity-fluctuation noise spectra, all acquired under the same laser operating conditions. The spectra were obtained from analysis of the output current of the detector (Fig. 4) with no input present, over a range of frequencies around 35 MHz (the separation of the transverse modes from the fundamental lasing mode). With no spatial filtering of the output, the noise spectrum appears flat, being dominated by the shot noise from the lasing mode. The origin of the noise was confirmed by checking that the noise power density varied linearly as the laser power was attenuated with neutral density filters. The other spectra in Fig. 9 reveal the effect of spatial filtering on the noise; in these cases half of the laser power is blocked by a blade aligned either vertically or horizontally. In Sec. IV (see Fig. 6) this was shown to satisfy the condition for optimizing the gain for a reinjected signal; the noise level is similarly maximized by this arrangement.

The data of Fig. 9 clearly reveal the noise cancellation that results from the orthogonality of the modes involved. For the two-lobe TEM_{01} and TEM_{10} modes discussed here, this implies that the spontaneous emission into one lobe is matched by an identical contribution into the other lobe, but that these two contributions are always π out of phase. Care must be taken in order to achieve the flat noise curve of Fig. 9; there must be no bias towards one or other of the two lobes in the detection process, as this will upset the delicate balance between the two halves and lead to incomplete cancellation. In our earlier publications I and II, we developed a theory for the intensity-fluctuation noise spectra, and it was shown both experimentally and theoretically that the gain and noise spectra were very closely related. While we make

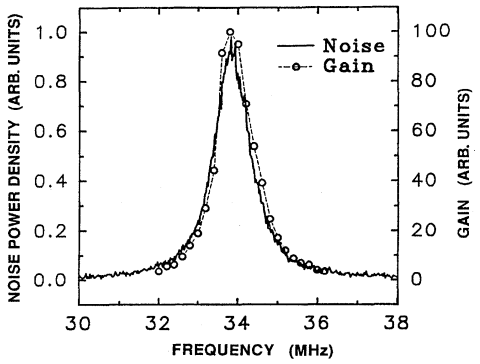

FIG. 10. An example of noise and gain profiles for the TEM_{10} mode, both measured at a laser power of 4.0 mW. These have been superimposed to show the close agreement demonstrating a fundamental property of amplifiers.

no attempt here to derive the corresponding theory for the subthreshold transverse modes, it nevertheless still holds true that the gain and noise remain intimately linked. This is illustrated in Fig. 10, where the noise spectrum is displayed superimposed on the gain profile, both measured under identical conditions. The close relationship between gain and noise was verified for both TEM_{01} and TEM_{10} states over a wide range of laser power; the noise spectra display the same shifts with changes of laser power as do the gain profiles and they also show a similar response to cavity perturbations.

Noise spectra very similar to those shown here are reported in [4] for a single-frequency krypton-ion laser. A split detector was used to optimize the noise power, by changing by π the relative phase of the contributions from the two lobes of the transverse mode under investigation. In this way, the contributions can be made to add, rather than cancel. In [4], the noise was interpreted as being caused by fluctuations in laser beam position due to the beating between the lasing mode and emission into the transverse modes, and the effect was given the name "stochastic position noise." However, it should be borne in mind that these fluctuations are small, representing a beam displacement of only a tiny fraction of its diameter. This reflects the fact that only a very small fraction of the total laser output is emitted into the subthreshold modes. For example, in the argon-ion laser studied here, this fraction is of order 10^{-7} at twice threshold pumping rate ($C=2$).

In our work, it was not possible to measure accurately the noise profiles at values of laser power higher than about 15 mW. This is because as the power is increased the laser output must be attenuated to avoid detector nonlinearity and damage. This reduces the signal-to-noise level of the noise spectra, until measurements become impossible without laborious averaging. On the other hand, the measurements of gain by reinjection described in Sec. IV do not suffer this constraint, demonstrating the versatility of this technique and its potential for laser diagnostics.

Finally, following this discussion of an increase in noise level after *spatial* filtering of the laser output, it is interesting to note that a similar phenomenon occurs after *spectrally* filtering the output [14]. The noise cancellation in this latter case has quite different origins: contributions due to spontaneous emission from opposite sides of the laser line are coupled by four-wave mixing.

VI. THEORETICAL AND EXPERIMENTAL STUDY OF CAVITY PERTURBATION

This section describes an investigation of the effects of cavity perturbation on the behavior of the subthreshold transverse modes. An experiment was performed to study the shift in transverse-mode frequency in the argon-ion laser induced by translating a straight knife edge across the cavity, positioned close to mirror $M1$ (see Fig. 1). The knife edge was aligned vertically and mounted on a micrometer stage to allow precise horizontal translation into the intracavity laser beam. This situation was also theoretically investigated by cavity modeling methods.

The experiment was carried out using the same reinjection technique described in detail in Sec. IV. Gain profiles were obtained as the offset frequency was tuned around the transverse-mode resonances, and the peak positions for these curves were then evaluated for different knife-edge positions. The TEM_{01} mode is relatively unaffected by this cavity perturbation: its lobes are aligned vertically, and so the mode can adapt relatively easily to the intrusion of the knife blade. However, for the TEM_{10} mode, its symmetry becomes significantly disturbed as soon as the knife edge begins to cut into its edge. The resulting shift in the peak gain frequency for the TEM_{10} mode is plotted in Fig. 11. This data set was obtained at an unperturbed laser power of 11.5 mW. The power level drops as the knife edge translates further into the cavity, until the laser is eventually extinguished.

To model the perturbed cavity we construct a complex round-trip propagation matrix for the Laguerre-Gaussian modes Ψ_{pq}, and numerically diagonalize it to extract the eigenvectors (transverse modes) and eigenvalues (losses and phase shifts). The computer model is derived from waveguide resonator studies [7,15]. In this earlier work the effect of a hollow dielectric waveguide was described by a matrix for coupling input Gaussian beams through the waveguide into a new basis of output Gaussian beams. The resonator problem was solved by setting up the round-trip matrix in terms of free-space basis modes (Laguerre-Gaussian or Hermite-Gaussian), or in terms of waveguide basis modes (LP_{nm} or EH_{mn} [7]), with the choice of basis (that is, of reference plane within the cavity) made for convenience but having no formal importance. Here, there is no waveguide (or a waveguide of zero length, i.e., a circular aperture), and by adjusting the limits of the overlap integrals we can find the coefficients in the nondiagonal coupling matrix which describes the effect of the combined mirror and knife edge.

This matrix approach [15,16] is equivalent to solving a set of simultaneous equations for the Laguerre-Gaussian mode amplitudes [17,18] and has often been described in the literature. We treat a passive resonator: the model is fully multimode, and predicts the relative frequencies of the fundamental and higher-order transverse modes of the (mechanically) perturbed cavity, but it does *not* solve rate equations or include microscopic effects of the active medium. We should also remark that the knife edge represents a severe perturbation, which strongly affects the transverse-

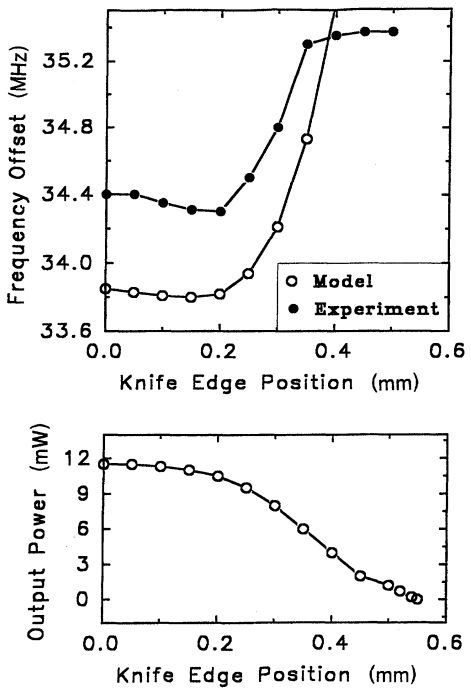

FIG. 11. Measurements on a perturbed laser cavity for the plane-concave mirror arrangement [case (i)]. The upper plot shows experimental data for the peak gain of the TEM_{10} mode: the frequency shifts as the knife blade translates into the cavity. The results of the model calculation are also plotted. The lower plot shows the reduction in laser output power as the knife blade obstructs the lasing mode.

mode shapes as well as their phase shifts, so that it would be unwise to assume constant values of the fractions f_L and f_T (Sec. III). Nonetheless, the results in Fig. 11 provide further interesting evidence that the autodyne techniques can be applied to real perturbed lasers and give reasonable agreement between theory and experiment.

Note that one possible source of discrepancy between the data and theoretical predictions of Fig. 11 is the apparent shift in mode frequency that results from the influence of population pulsations, as calculated and measured in Secs. III and IV, respectively (see Figs. 2, 7, and 8). This shift is, of course, dependent on laser power and so its value will vary as the cavity is perturbed and the laser power drops. For the mode considered here (with the same axial-mode number j as the lasing mode), the shift will be positive (adding to the offset), and its contribution will decrease as the laser power diminishes. A full quantitative correction of this effect is therefore likely to improve the agreement between theory and experiment in Fig. 11.

VII. EXPERIMENTAL TRACKING OF THE APPROACH TO THRESHOLD

In this section, we use the reinjection technique to monitor the gain behavior under a type of perturbation which favors a particular transverse mode compared to the lasing mode. The data obtained demonstrate our ability to monitor

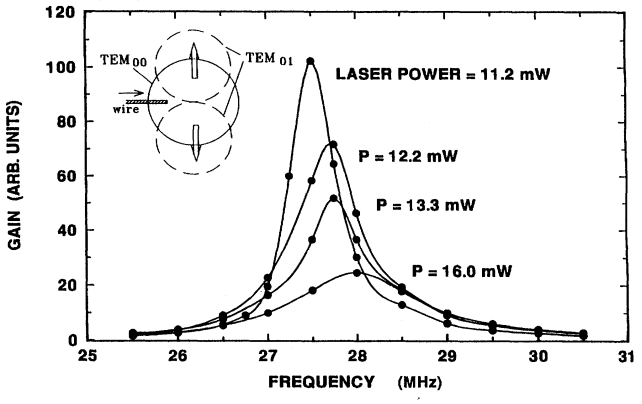

FIG. 12. Approach to threshold of TEM_{01} mode. As the horizontal wire penetrates further into the cavity, the laser power drops; this is indicated on each profile. Note also the slight shift that results from perturbing and distorting the modes of the cavity.

the approach of a subthreshold mode towards the lasing threshold. Figure 12 shows the effect on the gain curve for the TEM_{01} mode as a thin (~ 100 μm diameter) horizontal wire is progressively inserted further into the laser beam within the cavity. The wire is perpendicular to the laser axis, and is also accurately centered (see inset of Fig. 12). This configuration tends to favor the TEM_{01} mode, in comparison to the lasing TEM_{00} mode, because the wire lies along a null of the TEM_{01} field. Hence the losses incurred by the TEM_{00} mode are much greater than for TEM_{01}, and the laser output drops accordingly. This drop in laser power is accompanied by an increase in the population inversion, and the TEM_{01} mode is able to exploit this. As the wire penetrates further, the TEM_{01} mode acquires higher and higher gain with reduced bandwidth, eventually reaching threshold just beyond the setting for the narrowest curve in Fig. 12.

After the TEM_{01} mode has exceeded the threshold, it needs only a small extra translation of the wire to cause the TEM_{00} mode to be extinguished. However, there does exist a limited region where both TEM_{00} and TEM_{01} modes coexist. This may be contrasted with the behavior as the argon-ion laser hops between different longitudinal modes [19]. In that case, coexistence of two modes is not observed, as they share the same distribution of gain, and are in competition for exactly the same atoms: there can only be one winner.

VIII. CONCLUSIONS

We have presented laser amplifier equations of motion, including a first attempt at the inclusion of higher-order transverse modes, and solved these equations for some special cases. The results are in reasonable agreement with measurements of the mode spectrum of an argon-ion laser, both when the laser cavity is mechanically perturbed and when the pumping rate is varied. In particular, we have used a reinjection technique to probe the mode behavior and to track the mode eigenvalue (gain and phase shift) as threshold is approached and exceeded. We have compared the measured relative frequency shifts of higher-order subthreshold modes, when we apply the gross perturbation of a straight-

edge aperture at one mirror, with the results of a multimode matrix computer model.

The studies reported here can easily be extended to investigate some of the yet higher-order transverse modes. For example, the detection of a quadrant of the output laser beam enhances the beat gain for the four-lobe TEM_{11} mode. A resonance confirming the presence of this mode was clearly detected at approximately twice the frequency offset of the TEM_{01} and TEM_{10} modes. We have also carried out a brief investigation of the gain experienced by the beam reflected from the cavity. These gain profiles display the same resonant features as those in transmission, with the important difference that at large detunings from resonance the gain becomes unity, rather than tending to zero as in transmission measurements. A full evaluation of this technique is necessary to assess the potential of the reinjection methods reported here for investigation of single-ended lasers.

The reinjection method (related to the self-aligning "autodyne" technique in coherent laser radar referred to in I) shows promise for optimizing laser performance via measurements that have previously been rather difficult. The appearance and development of significant subthreshold modes can be studied, and combined in principle with real-time adjustments, so that spurious laser frequencies (that might imperil coherent lidar operation) can be identified and avoided. There is also increasing interest in the use of autodyning directly in lidar systems, where the light scattered from a target is reinjected and amplified within the laser source.

ACKNOWLEDGMENTS

C.J.S. is funded by a MOD research agreement with the University of Essex. We also wish to acknowledge the assistance of G. D. Lewis, P. R. Tapster, and E. Jakeman of DRA Malvern.

[1] M. Harris, C. A. Hill, and J. M. Vaughan, Electron. Lett. **29**, 997 (1993).

[2] R. Loudon, M. Harris, T. J. Shepherd, and J. M. Vaughan, Phys. Rev. A **48**, 681 (1993).

[3] R. Loudon, C. J. Shackleton, M. Harris, T. J. Shepherd, and J. M. Vaughan, Phys. Rev. A **50**, 658 (1994).

[4] M. D. Levenson, W. H. Richardson, and S. H. Perlmutter, Opt. Lett. **14**, 779 (1989); in *Quantum Optics V*, edited by J. D. Harvey and D. F. Walls (Springer-Verlag, Berlin, 1989).

[5] H. Kogelnik and T. Li, Appl. Opt. **5**, 1550 (1966).

[6] A. E. Siegman, *Lasers* (University Science Books, Mill Valley, CA, 1986).

[7] C. A. Hill, in *The Physics and Technology of Laser Resonators*, edited by D. R. Hall and P. E. Jackson (Adam Hilger, Bristol, 1989).

[8] For an introduction to the concept of biorthogonality, see Chap. 21 of [6].

[9] M. Harris, R. Loudon, T. J. Shepherd, and J. M. Vaughan, Opt. Commun. **91**, 383 (1992).

[10] M. Harris, R. Loudon, G. L. Mander, and J. M. Vaughan, Phys. Rev. Lett. **67**, 1743 (1991).

[11] G. N. Pearson, M. Harris, C. A. Hill, J. M. Vaughan, and A. M. Hornby, IEEE J. Quantum Electron. **31**, 1064 (1995).

[12] D. C. Hanna, IEEE J. Quantum Electron. **5**, 483 (1969).

[13] M. Sargent, M. O. Scully, and W. E. Lamb, *Laser Physics* (Addison-Wesley, Reading, MA, 1974).

[14] M. Harris, R. Loudon, T. J. Shepherd, and J. M. Vaughan, Phys. Rev. Lett. **69**, 2360 (1992).

[15] C. A. Hill and A. D. Colley, IEEE J. Quantum Electron. **26**, 323 (1990).

[16] J. Degnan and D. R. Hall, IEEE J. Quantum Electron. **9**, 901 (1973).

[17] G. Stephan and M. Trümper, Phys. Rev. A **28**, 2344 (1983).

[18] L. Y. Wang and G. Stephan, J. Mod. Opt. **30**, 1899 (1991).

[19] M. Harris, R. Loudon, T. J. Shepherd, and J. M. Vaughan, Opt. Commun. **101**, 432 (1993).